ELSEVIER

Journal of Biomechanics 35 (2002) 189–198

JOURNAL OF BIOMECHANICS

www.elsevier.com/locate/jbiomech
www.JBiomech.com

Microstructural elasticity and regional heterogeneity in human femoral bone of various ages examined by nano-indentation

J.Y. Rho[a], P. Zioupos[b,*], J.D. Currey[c], G.M. Pharr[d,e]

[a] Department of Biomedical Engineering, University of Memphis, Memphis, TN 38152, USA
[b] Department of Materials and Medical Sciences, Cranfield University, Shrivenham SN6 8LA, UK
[c] Department of Biology, University of York, P.O. Box 373, York YO10 5YW, UK
[d] Department of Material Sciences, University of Tennessee, Knoxville, TN, USA
[e] Metals and Ceramics Division, Oak Ridge National Laboratory, Oak Ridge, TN 37831, USA

Accepted 22 September 2001

Abstract

The elastic modulus and hardness of secondary osteonal and interstitial bone was examined through the thickness of the cortex of human femora of various ages by nano-indentation. There was a clear difference between the stiffness and hardness of secondary osteonal and interstitial bone, the latter being stiffer ($F_{1,48} = 56.0$, $P<0.001$). There were some differences between the bones of different subjects; however, there were no differences that could be reliably associated with the chronological age of the subject, or with differences in location through the thickness of the cortex ($F_{2,48} = 0.21$, $P = 0.810$). Previous studies have been equivocal in relating changes in the macroscopic 'composite' material stiffness of bone to the age of the individual. By combining the results of the nano-tests with histological measures, we were able to produce a good relationship of the microstructural properties at the matrix level with the bending modulus of whole bone ($R^2 = 0.88$, $P<0.001$) and this improved further by taking into account the age of the individual ($R^2 = 0.94$, $P<0.001$). Our results suggest that using differences in the volumetric proportions of secondary osteons versus interstitial bone, and the properties of these elements/structures in isolation may be a more accurate method of determining differences in elastic modulus of whole bone between individuals of various ages. © 2002 Elsevier Science Ltd. All rights reserved.

Keywords: Secondary osteons; Interstitial bone; Nano-indentation; Age

1. Introduction

There have been a number of studies examining the mechanical behaviour of human cortical bone with increasing age. It has been shown that after maturity stress and strain at failure in human bone reduce (Lindahl and Lindgren, 1967; Yamada, 1970; Burstein et al., 1976; Evans, 1976; Smith and Smith, 1976; Wall et al., 1979; McCalden et al., 1993; Martin, 1993). The toughness also declines with age (Courtney et al., 1996; Currey et al., 1996; Zioupos et al., 1998, 1999). However, the results are varied for elastic modulus in adults, some workers finding an increase, some a decrease with age (Burstein et al., 1976; Evans, 1976; McCalden et al., 1993; Martin, 1993; Zioupos and Currey, 1998).

Bone material is non-uniform and heterogeneous and at any moment comprises a collection of elements of older or younger 'tissue' age. An increase in 'tissue' age brings about increased mineralisation (Grynpas, 1993) and local hypermineralised regions have a tendency to crack easily and therefore, affect the ultimate mechanical properties of the whole bone tissue (Boyce and Bloebaum, 1993). The effects of this mineralisation pattern are more complex than the effects observed when the overall mineral content of a tissue increases (Currey, 1982, 1988; Chakkalakal et al., 1990). When the overall mineral content increases bone becomes stiffer and stronger (as in early maturation up to the age of 35, at least in bending mode) and there may be a point of optimum mineralisation, whereby when a certain mineralisation threshold is exceeded bone becomes weaker. Because of the difference between 'tissue' and 'chronological age', and also between global and local mineralisation it is unknown how local

*Corresponding author. Tel.: +44-1793-785932; fax: +44-1793-785772.
E-mail address: zioupos@rmcs.cranfield.ac.uk (P. Zioupos).

0021-9290/02/$ - see front matter © 2002 Elsevier Science Ltd. All rights reserved.
PII: S0021-9290(01)00199-3

mineralisation patterns affect the bulk mechanical properties of ageing bone (Martin, 1993). For strength and toughness, in particular, there may be other material changes, which degrade the mechanical quality of the bone (Simmons et al., 1991; Zioupos et al., 1999; Bailey et al., 1999).

Some acoustic methods which have been applied at both the macroscopic and the microscopic level (Ashman and Rho, 1988, Ashman et al., 1989; Rho et al., 1993; Katz and Meunier, 1993) are suitable for examination of regional variations in the mechanical properties of bone, but these are fraught by various experimental problems. Detailed structural information may be obtained from optical microscopy, X-ray diffraction, and electron microscopy, but gives no mechanical information. Backscattered electron (BSE) imaging (Skedros et al., 1993; Bloebaum et al., 1997) allows microscopic observations of mineralisation over a larger sample area without simultaneously providing any data for the stiffness, strength or hardness of the tissue. In contrast, nano-indentation is a mechanical micro-probe method which allows the direct simultaneous measurement of elastic modulus and hardness, with a spatial resolution in some cases of better than 1 μm. Such a resolution (provided that the breadth and associated depth of indentations is smaller than the size of the structures of interest) may allow the direct measurement of bone properties at, for instance, the lamellar level. The effects of various pathophysiological conditions, and in some cases ageing can, therefore, be examined at both the microscopic and the macroscopic level. Here, by using the nano-indentation technique on mature bone (of individuals over 35 years old) we aim to address the following questions: (i) Do the osteonal and interstitial bone properties change as a function of age? (ii) Do these same properties change as a function of the radial direction through the cortex? (iii) Can the micromechanical differences we observe by nano-indentation be directly related to the elastic behaviour of whole bone tissue? (iv) Can any other structural information be combined with the nano-indentation data to explain the combined effects of mineralisation and remodelling in the ageing bone matrix? Knowledge of the fine biomechanical properties of bone, and how these affect the bulk tissue, may provide insight into the nature of bone changes and also for the extent to which these changes differ in different parts of the bone and in relation to the age of an individual.

2. Materials and methods

Specimens were obtained from human femoral bone of nine male subjects aged 35–95 years who had died suddenly, had not been hospitalised and whose bone condition were not related to the cause of death. These bones have already been biomechanically characterised (Zioupos and Currey, 1998) in terms of their elastic modulus E, bending strength S_f and fracture toughness (K_C, *J–integral*, work of fracture W_f) using specimens of three different geometries (Fig. 1). Both the previous and the present study include only men in order to avoid the consequences of the changes that take place in women after menopause.

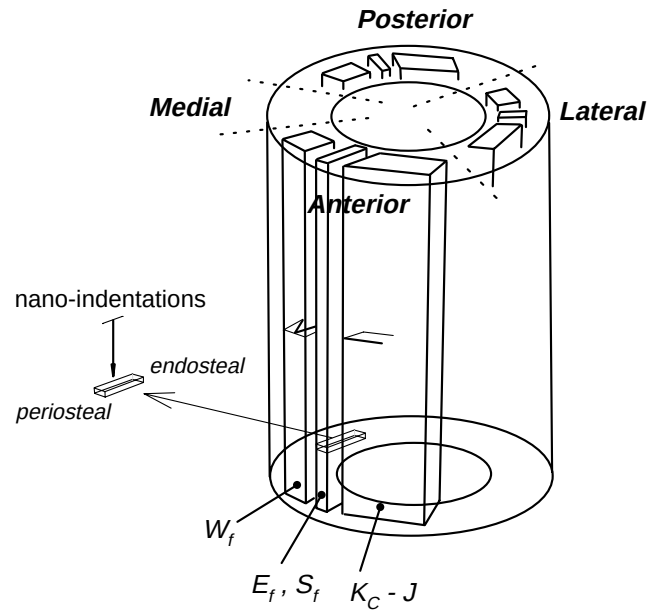

Fig. 1. Sections for nano-indentation (roughly $2 \times 2 \times 6\,mm^3$) were cut transversely from the ends of plate-like mechanical specimens, which were used to measure E and S_f from the anterior sector of the bones. The indentations were normal to the two transverse surfaces of the sections. The geometry, design and location of other specimens that were used to derive the average bending values for the stiffness, strength and toughness of the bone in a previous study by Zioupos and Currey (1998) is also shown.

2.1. Nano-indentation measurements

Transverse sections with a depth of <2 mm, a width of ~ 2 mm, and a length of ~ 6 mm were cut from the plate-like mechanical specimens (which were used to measure E and S_f) from just one sector (anterior) of the bones (Fig. 1). The specimen were dehydrated in a series of alcohol baths and embedded without vacuum in epoxy resin at room temperature. This standard procedure mounts the specimen securely so as to allow the very sensitive nano-indentation procedure to take place. The resin does not alter the nature of the bone neither does it filter into its various cavities; it simply encapsulates each bone sample. All specimens were subjected to exactly the same cleaning and mounting protocol simultaneously and they were all embedded in a single resin block. The embedded specimens were afterwards ground using silicon carbide abrasive papers

of decreasing grit size (600, 800, and 1200 grit) under deionized water and metallographically polished on microcloths with successively finer grades of alumina powder to the finest, 0.05 μm, grit to produce the mirror smooth surfaces needed for testing by nano-indentation.

Nano-indentation tests were conducted by using a Berkovich diamond indentor, in load control testing. All tests were carried out in dry room temperature conditions in the single block that contained all specimens, and therefore, specimens of all ages were examined in identical testing and ambient conditions. The indentor was loaded and unloaded, with two intervening periods during which the load was held constant. To minimise the effects of viscoelasticity and creep on property measurements, a relatively long constant load hold period was introduced before the final unloading. During this time the viscoelastic deformation became negligible. The second constant load hold period, near the end of the test, at 10% of the peak load, was used to establish the rate of thermal expansion or contraction of the testing apparatus, to correct the displacement data for thermal drift. Viscoelastic recovery was significant during the first portion of the hold period, but after about 200 s the viscoelastic effects became small compared to the thermal effects. Data from the last 100 s of the second hold period were used to establish the thermal drift rate and correct the displacement data.

The nano-indentation test imposed a maximum load of 8 mN, with a loading rate of 400 μN/s, which in bone produces hardness impressions with depths of about 700 nm. The hardness and elastic modulus for each indentation was determined by using the well documented method of Oliver and Pharr (1992), which we will only describe here very briefly. The quantities of concern include the peak load $P_{\max}$, the contact area A_c, and the contact stiffness S. The equations used to compute the hardness (H), and the effective indentation modulus (E_{eff}) from the measured quantities are:

$$H = \frac{P_{max}}{A_c}, \tag{1}$$

and

$$E_{\text{eff}} = \frac{\sqrt{\pi}}{2}\frac{S}{\sqrt{A_c}}. \tag{2}$$

The E_{eff}, the effective modulus for the indentor–specimen combination, is also equal to

$$E_{\text{eff}} = \left[\frac{1-v_s^2}{E_s} + \frac{1-v_i^2}{E_i}\right]^{-1}, \tag{3}$$

where v is the Poisson's ratio and the subscripts s and i refer to the sample and the indentor, respectively. The known elastic properties of the diamond indentor were $v_i = 0.07$ and $E_i = 1140$ GPa, and the assumed Poisson's ratio for bone was $v_s = 0.30$. The elastic modulus for the specimen (E_s) is derived from the stiffness data using Eqs. (2) and (3). Eq. (2) is derived making the assumption that the tested material is elastically homogeneous and isotropic. When used to measure the elastic modulus of an anisotropic material, such as bone, the modulus derived from this equation is an unknown weighted average of the anisotropic elastic constants (Rho et al., 1997, 2000; Zysset et al., 2000). Fused silica, which exhibits elastic isotropy and has a relatively low modulus-to-hardness ratio, and single crystal aluminum, which is more ductile, were used to calibrate the tip shape function. The elastic modulus measured for these two standards was 72.1 ± 0.5 and 70.05 ± 1.54 (GPa $\pm$ S.D.) very close to the canonical values of 72.0 and 70.0 GPa, respectively, showing that the machine was properly calibrated.

In total, 486 indentations were made. Three target areas (from near the centre of the specimen along the radial direction) comprising an osteon and a nearby interstitial packet of bone were selected in each of the endosteal, middle and periosteal sites of the specimens (nine regions = target areas in each specimen). Six sites were examined in each target area. Of these three sites were in lamellae of an osteon and three in lamellae in the nearby interstitial region (Fig. 2). The word 'lamella' is used here to indicate that we targeted the measurements at the centre of what is generally called the 'thick' osteonal lamellae of bone's microstructure (Rho et al., 1999). However, due to the size of the actual impressions it is by no means certain that the deforming volume was confined within the thick lamellar boundaries, nor we intend it to be (given the substantial difference in lamellar properties that may exist between 'thick' and thin' lamellae, Hengsberger et al., 2000). The aim here is to derive microstructural and not necessarily lamellar characteristics. It is also always important to distinguish primary osteons from secondary osteons/Haversian systems (Currey, 1982); we shall, in this paper use the term 'osteons' and 'osteonal' in relation to secondary osteons. The position of each indent was selected manually to find the desired location on the centre of lamellae and thus avoiding cell lacunae or areas of irregular microporosity. It is known that there may be small variations in the nano-indentation values with radial distance within single osteons (Rho et al., 1999), so we standardised our protocol, applying to all samples the same loading time sequence, approximately the same probe site (≈ 60 μm from the centre of the osteon) and mounting all sections in a single resin block. The average value of the three indents made in each osteonal and interstitial site is given in Table 1 and these values are the ones used in subsequent analysis.

2.2. Whole bone elasticity measurements

The sections for nano-indentation were cut from larger test specimens, whose biomechanical properties

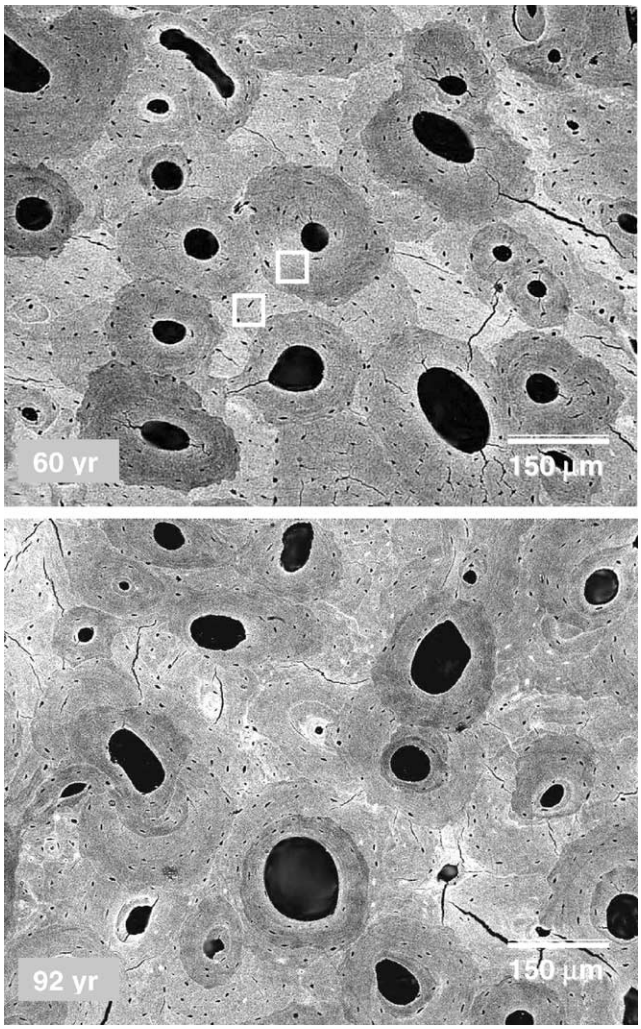

Fig. 2. Back-scattered scanning electron micrographs produced for the 60-year-old and the 92-year-old males of this study in carbon coated sections (at 25 kV). Darker areas are those that have been more recently remodelled and contain relatively lower mineral content. 'Older' interstitial tissue areas appear lighter; they are more highly mineralised (higher yield of electrons = higher mineral density). The two boxes show where roughly a group of nano-indentations (not visible at this scale) in nearby osteonal and interstitial areas, would appear.

had been measured previously (Zioupos and Currey, 1998) in a purpose-built bath for testing in 3-point bending in Ringer's at 37°C. Plate-like specimens were used to measure the elastic modulus in flexion E in the linearly elastic region of the bone's stress/strain behaviour. The plate-like samples were aligned with their width on a longitudinal/radial plane and therefore each specimen contained a cross section stretching from the inner endosteal regions to the sub-periosteal regions (Fig. 1) producing an average bending modulus value in the radial direction. As for other mechanical properties three specimens were used to derive an average value as the best estimate for the bending modulus of elasticity of the femoral bone of each individual of this study. The reason for averaging is that as we have already found (Zioupos and Currey, 1998; Zioupos, 2001): (i) there is no evidence that the three values (for any mechanical, physical or histological property) vary in any systematic way round the bone and/or as a function of age of individuals and (ii) each measurement is accompanied by an experimental error which is minimised by having more data.

2.3. Porosity measurements

In order to relate the bulk properties of whole bone to the nano-indentation values we also measured the different proportions of *secondary osteonal* and *interstitial* tissue, and also the *porosity* of the tissue. Sections, about 500 μm thick, were cut 2 mm behind the fracture surface of all three W_f specimens (Fig. 1) at each age by the use of an EXAKT precision band saw. The sections were thinned down to 200 μm, cleaned with a 2:1 chloroform/methanol mixture and then ultrasonicated in a water bath. The sections were stained with toluidine blue and fast green to enhance the recognition of the structural elements and were left to dry out overnight at 37°C. The sections were mounted between a glass slide and a glass cover slip surrounded by RUBERT Acrulite® Microtech type-A resin mixed with black carbon powder. When the casting mixture had hardened the glass cover slip was removed and the mounted sections were polished carefully on one side by 1200 grade carborundum paper and alumina paste to a mirror finish. Using a JOYCE LOEBL Magiscan© image analysis system an estimate of the porosity of the specimen was made as the fraction of the compact bone area to the area of the cavities (cavities included blood channels and erosion spaces, but not osteocyte lacunae or canaliculi). The image was firstly thresholded according to grey level and then, if necessary, was corrected by hand by use of a 'touch up pen' on the screen (Currey, 1988; Zioupos et al., 1996). The method was applied consistently across the various ages (individuals). Porosity was turned into volume fraction $V_f = (1 - porosity)$ to express the compact bone area that is actually present as a fraction of the overall cross-sectional area.

2.4. Secondary osteonal area

The average area occupied by secondary remodelling osteons was measured by one observer (P.Z.) for all specimens (there were three samples at each age, each sample was measured three times, and the data averaged). Secondary osteons were distinguished from primary osteons by the use of a number of helpful features: (i) the grey level of these remodelled parts of the bone, this was aided by the heavier staining by the histological dyes since these osteons have a lower mineral/organic ratio; (ii) their broader central Haver-

Table 1
Elastic moduli and hardness values (second entry in italics) for the osteonal and interstitial sites. Each value is the mean of three indentations in GPa (mean ± standard deviations)

Age		Endosteal		Middle		Periosteal	
		Osteonal	Interstitial	Osteonal	Interstitial	Osteonal	Interstitial
35		22.8±2.4	25.0±0.9	23.4±0.9	24.9±0.6	22.5±0.7	23.8±1.1
	35	*0.61±0.10*	*0.68±0.02*	*0.64±0.05*	*0.69±0.01*	*0.60±0.06*	*0.68±0.06*
42		22.2±0.3	24.4±1.2	21.9±0.2	24.7±1.9	21.1±1.2	23.7±1.1
	42	*0.60±0.01*	*0.69±0.05*	*0.58±0.02*	*0.70±0.07*	*0.58±0.08*	*0.66±0.02*
46		20.3±2.3	23.5±1.0	18.8±0.7	23.2±0.8	19.5±1.1	23.5±0.9
	46	*0.60±0.02*	*0.72±0.02*	*0.53±0.01*	*0.72±0.03*	*0.56±0.02*	*0.65±0.04*
48		23.1±1.0	25.3±0.9	23.6±1.5	24.4±0.6	21.0±0.7	24.4±1.2
	48	*0.64±0.05*	*0.72±0.06*	*0.68±0.05*	*0.68±0.01*	*0.55±0.03*	*0.71±0.05*
50		22.0±1.7	24.2±1.7	21.4±3.3	23.5±2.0	21.6±1.5	24.5±0.7
	50	*0.57±0.06*	*0.63±0.07*	*0.52±0.09*	*0.66±0.07*	*0.58±0.06*	*0.68±0.02*
52		21.6±0.9	24.1±0.9	21.8±0.3	21.6±3.8	21.9±1.6	22.5±1.2
	52	*0.60±0.03*	*0.68±0.06*	*0.64±0.03*	*0.67±0.12*	*0.63±0.01*	*0.68±0.03*
60		19.8±1.4	24.9±1.1	22.1±2.4	25.1±0.8	22.4±0.3	25.3±2.1
	60	*0.50±0.06*	*0.68±0.04*	*0.59±0.12*	*0.71±0.02*	*0.58±0.04*	*0.70±0.09*
70		22.9±1.2	23.6±1.0	22.1±3.1	23.6±1.1	22.7±1.0	25.1±0.8
	70	*0.64±0.06*	*0.65±0.04*	*0.62±0.10*	*0.69±0.07*	*0.64±0.05*	*0.72±0.03*
92		20.5±0.9	22.4±2.8	20.8±1.0	23.3±0.5	23.8±2.2	25.3±1.2
	92	*0.57±0.03*	*0.70±0.07*	*0.58±0.04*	*0.68±0.02*	*0.67±0.08*	*0.74±0.05*
Average:		21.7±1.7	24.1±1.5	21.8±2.1	23.8±1.8	21.8±1.6	24.3±1.4
Average:		*0.59±0.06*	*0.68±0.05*	*0.60±0.07*	*0.69±0.05*	*0.60±0.06*	*0.69±0.05*

sian canal; (iii) the distinct cement line oundary; (iv) their relatively less regular cylindrical border; (v) their encroachment into other primary osteons and remnants of woven/lamellar matrix, which were of an older tissue age. The measuring technique employed first a thresholding according to grey level and then manually (touch up pen) correcting for artefacts. The total area of the secondary osteons divided by the total nominal cross-sectional area derived the un-corrected secondary osteonal area (*SecOsAr*) fraction. This can be further corrected for the actual solid load bearing area of these osteons if the area occupied by the central Haversian canals and the general porosity of the tissue is accounted for and excluded from the calculation (McCalden et al., 1993).

3. Results and analysis

A summary of the elastic moduli (E) and hardness (H) values of the osteonal and interstitial bone sites as determined by nano-indentation is given in Table 1. There was overall a fairly good relationship between the associated elastic modulus predictions and the hardness data derived from each indentation ($R^2 = 0.73$). Unlike conventional indentation techniques, in which the hardness values have to be independently related to the material stiffness by separate mechanical tests, nano-indentation by its very nature derives both these measurements together. In the results and discussion that follow we make use primarily of the modulus data in the knowledge that hardness behaves in a very similar manner.

3.1. Elastic modulus

The effects we seek to explore here are: (a) the difference between osteonal and interstitial bone stiffness, (b) the inter-subject variability and (c) any trends with age.

Osteonal bone versus *interstitial bone:* Table 1 and Fig. 3 show a clear and consistent difference between the stiffness of the bone in the osteons and in the surrounding interstitial bone. Of the 27 comparisons that can be made, all but one (Table 1, middle/52-year old) have the interstitial bone stiffer than the osteonal bone. In the one 'odd' comparison still the corresponding hardness value for the nearby interstitial tissue is higher than the osteonal tissue. Analysis of variance showed that the position in the cortex (endosteal, middle or periosteal) was not a significant factor ($F_{2,48} = 0.21$, $P = 0.810$), while the site (either in the osteon or in the interstitial packet) was extremely important ($F_{1,48} = 56.0$, $P < 0.001$).

Differences between bones: Analysis of variance for elastic modulus with respect to bone number (coded arbitrarily) and position within the section (endosteal, mid or periosteal), both considered as factors, showed that for osteonal bone the position was not significant ($F_{2,16} = 0.04$, $P = 0.957$) but there was a (just signifi-

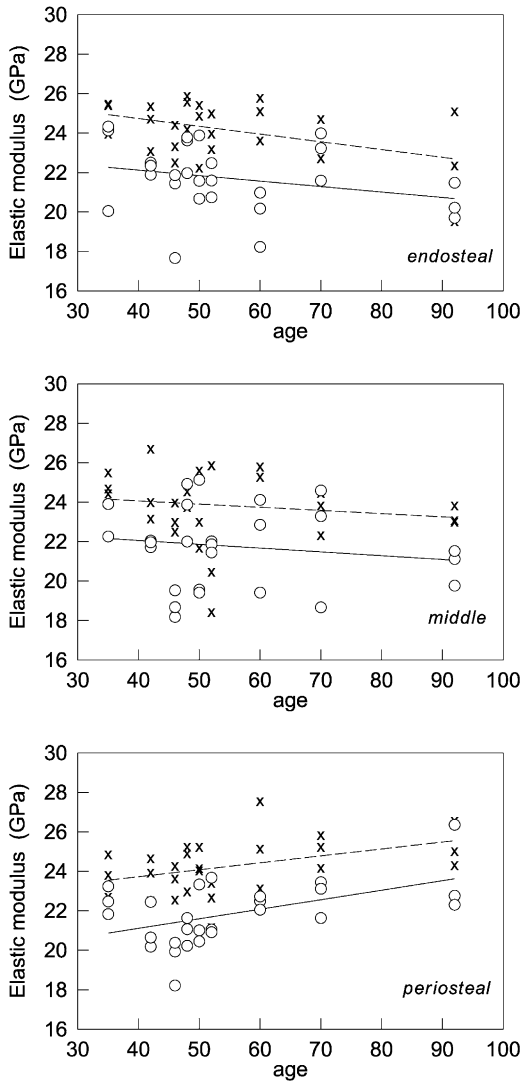

Fig. 3. The elastic modulus versus age data for osteonal (○) and interstitial (×) sites for the three positions in the cortex. Linear regression lines are shown dashed (interstitial) and solid (osteonal).

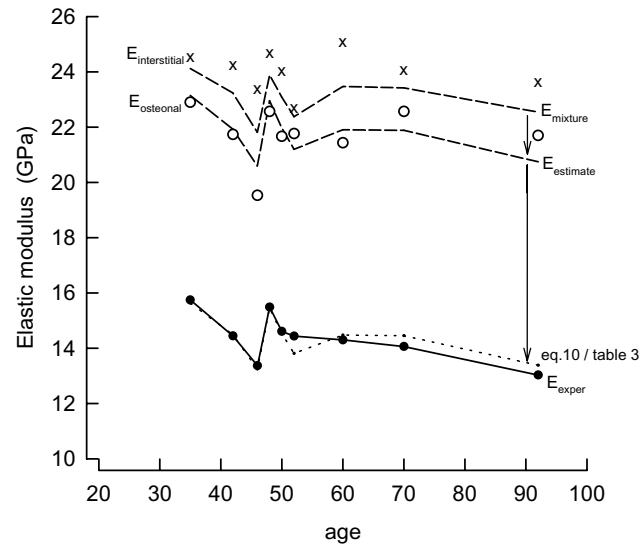

Fig. 4. Successive approximations (dashed lines) by producing from the original data (Table 2) for osteons (○) and interstitial bone (×) the variables: E_{mixture} and E_{estimate}. Finally the output of the regression Eq. (10) (dotted line) is compared to the actual bending modulus data for the bone of the mid-diaphysis of the femur for the nine donors (solid symbols and line). Being able to follow variations in the micromechanical properties of individual structures, their relative volume fractions and the degree of porosity in the bone cortex produces a very good approximation of the actual macromechanical material stiffness of bone of various ages.

cant) difference between bones ($F_{8,16} = 2.68$, $P = 0.044$). (Inspection of Fig. 4 shows that the in-between bones variation was caused mainly by the specimen from the 46-year old individual.) Analysis of variance for elastic modulus of the interstitial sites showed that there was no effect of either the position ($F_{2,16} = 0.67$, $P = 0.525$) or the bone ($F_{8,16} = 2.30$, $P = 0.075$).

Age trends: Fig. 4 suggests that there were overall some small trends with age, both in osteonal and in the interstitial sites. The endosteal and middle regions showed a slight decline in osteonal and interstitial stiffness with age, while the periosteal side showed an increase with age. However, statistics could only confirm this case in two out of six possible combinations of slopes (three positions in the cortex and two tissue types): the trends for the endosteal interstitial bone sites ($R^2 = 0.55$, $P = 0.021$) and that for the periosteal osteonal bone sites ($R^2 = 0.45$, $P = 0.050$).

3.2. Relationship between whole bone stiffness and nano-indentation

The nano-indentation specimens came from three areas through the thickness of the anterior cortex, and came from both osteonal and interstitial tissue. We have compared the means of these values from the three areas, keeping osteonal (NanoE_{osteons}) and interstitial (Nano$E_{\text{interstitial}}$) tissue separate, with the bending values for the elasticity of the whole bone (E_{exper}). We have also made the comparison by lumping all the nano-indentation values together, whether they came from osteonal or interstitial areas (NanoE_{average}). Table 2 includes the data for bone age, modulus (E_{exper}), porosity, SecOsAr (secondary osteonal area) and the nano-indentation values produced for the two tissue types (NanoE_{osteons}, Nano$E_{\text{interstitial}}$ and NanoE_{average}).

In Table 3 we give the least squares linear regressions of the E_{exper} by use of various explanatory variables. The relationships between the interstitial (Nano$E_{\text{interstitial}}$, Eq. (4)) values and the nano-indentation values for the osteons (NanoE_{osteons}, Eq. (5)) with the bending bone modulus (E_{exper}) were not significant ($P = 0.186$ and 0.053, respectively).

Table 2
Age, Young's modulus in bending—E_{exper}, porosity, and the relative area occupied by secondary osteons, of the present analysis for the mid-diaphysis bone from the femora of nine male donors (the three values are: the average of three measurements at the mid-diaphysis level, the value obtained in the anterior cortex and the standard deviation). Also, the nano-hardness elastic modulus of the osteonal (Nano$E_{osteons}$) and interstitial (Nano$E_{interstitial}$) sites, and their average (Nano$E_{average}$)

Age	E_{exper}	Porosity × 100	SecOsAr × 100	Nano$E_{osteons}$	Nano$E_{interstitial}$	Nano$E_{average}$
	(GPa)	(%)	(%)	(GPa)	(GPa)	(GPa)
35	15.8, 14.8, 1.4	4.1, 2.4, 1.4	26.8, 20.0, 7.1	22.9	24.6	23.7
42	14.5, 15.2, 0.6	5.7, 6.3, 0.6	40.9, 48.7, 6.9	21.7	24.3	23.0
46	13.4, 12.7, 0.9	5.6, 6.1, 0.5	41.1, 31.9, 8.1	19.5	23.4	21.5
48	15.5, 16.5, 1.1	3.9, 4.1, 0.2	38.3, 35.5, 8.7	22.6	24.7	23.6
50	14.6, 14.6, 0.1	4.9, 4.7, 1.0	40.6, 41.2, 2.0	21.7	24.1	22.9
52	14.4, 14.4, 0.5	5.3, 4.1, 1.8	36.8, 28.6, 9.7	21.8	22.7	22.3
60	14.3, 13.4, 0.8	6.7, 8.1, 2.4	44.5, 50.7, 5.4	21.4	25.1	23.3
70	14.1, 13.6, 0.6	6.6, 6.8, 1.2	44.6, 51.5, 10.9	22.6	24.1	23.3
92	13.0, 10.6, 2.1	8.0, 7.0, 1.9	57.5, 53.8, 8.1	21.7	23.7	22.7

Table 3
Linear regressions of E_{exper} using various explanatory variables, their R^2 values, the level of statistical significance P for the ANOVA, and the equation number[a]

	R^2	P	Equation
$E_{exper} = 0.20 + 0.590\text{Nano}E_{interstitial}$	0.24	0.186	4
(−5.1) (+0.793)	(0.12)	(0.372)	
$E_{exper} = 1.54 + 0.590\text{Nano}E_{osteons}$	0.44	0.053	5
(−2.5) (+0.757)	(0.20)	(0.234)	
$E_{exper} = -5.16 + 0.853\text{Nano}E_{average}$	0.49	0.037*	6
(−11.5) (+1.11)	(0.22)	(0.198)	
$E_{exper} = 18.1 - 8.93\text{SecOsAr}$	0.68	0.006*	7
(+16.4) (−6.02)	(0.18)	(0.254)	
$E_{exper} = -39.3 + 56.9V_f$	0.72	0.004*	8
(−37.2) (+54.2)	(0.34)	(0.102)	
$E_{exper} = -7.43 + 0.944E_{mixture}$	0.64	0.009*	9
(−20.7) (+1.50)	(0.36)	(0.089)	
$E_{exper} = -6.05 + 0.937E_{estimate}$	0.88	<0.001*	10
(−13.3) (+1.25)	(0.46)	(0.044)*	
$E_{exper} = -2.01 + 0.789E_{estimate} - 0.015$'age'	0.94	<0.001*	11
(+1.6) (+0.707) (−0.055)	(0.69)	(0.029)*	

[a] The values in parenthesis are produced by using for each variable just a single value obtained in the anterior cortex and as expected these derive weaker correlations. *Note that from Eq. (7) onwards the relationships attain significance and that in Eq. (11) where 'age' has been added as an extra explanatory variable the R^2 rises remarkably to 0.94 (0.69).

Eqs. (7) and (8) in the same table show the effect of the two architectural and structural properties we have also measured: SecOsAr, relative area occupied by secondary osteons and V_f the volume fraction (1−porosity). It is known from other studies that these variables can significantly affect the elastic modulus of bone (Currey, 1988; McCalden et al., 1993; Martin and Boardman, 1993) and that is the case here. Both Eqs. (7) and (8) are highly significant and of considerable predictive value ($R^2 = 0.68$ and 0.72, respectively).

The next logical step is to combine the two kinds of data: the structural variables on one hand and the micromechanical ones on the other. We have found that there are clear differences between the nano-indentation values for elastic modulus from the osteons and the interstitial sites, the modulus of elasticity for interstitial sites being on average 2.3 GPa higher than that for the osteonal sites. If the area proportions of these two tissue types differ considerably between bone of various ages (which they do, see SecOsAr, Table 2), then the value for E_{exper} should be better predicted by taking the area fraction of each tissue type, multiplying by its value for elastic modulus determined by nano-indentation, and adding them. This implies a simple rule of mixtures as used in composites: [SecOsAr$\times E_{osteons}$+(1 − SecOsAr)$\times E_{interstitial}$]. We call this variable '$E_{mixture}$' and it incorporates the micromechanical values into a combined relationship with SecOsAr increasing the $R^2 = 0.64$ (Eq. (9)). If we further incorporate the effect of volume fraction (an expression of the relative proportion of a solid phase being present) we produce a new variable; '$E_{estimate}$' $= E_{mixture} \times V_f$. Using this variable we obtain Eq. (10), which has an $R^2 = 0.88$ and is highly statistically significant ($P < 0.001$). Fig. 4 shows this step-by-step approximation of the bulk mechanical data values by taking into account progressively the nano-values of osteonal and interstitial moduli with their volume fractions and the porosity of the structure.

As a final model we include in Table 3 (Eq. (11)) a linear regression where 'age' has been added as a separate explanatory variable. The fit is now good, and shows, not surprisingly, that the variables we have measured here are not the only things that may change with age; there are many changes that we have been unable to measure. Eq. (11) shows that when age is included both variables '$E_{estimate}$' and 'age' are significant at $P = 0.001$ and $P = 0.05$, respectively. The amount of unexplained variance in the data is sharply reduced the R^2 increasing from 0.88 to 0.94

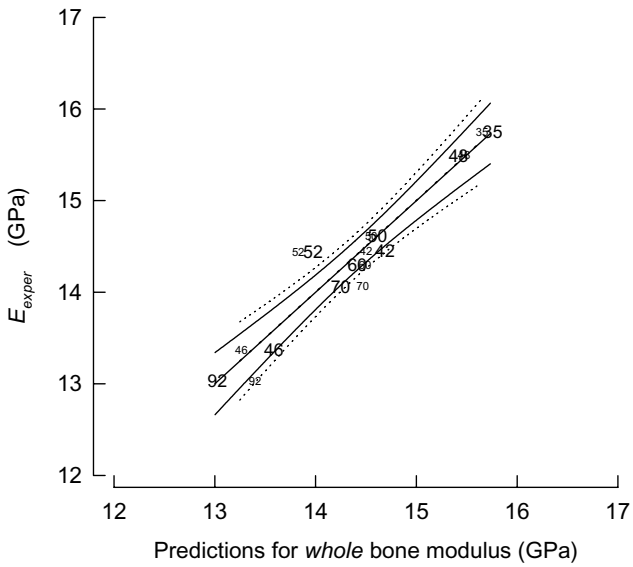

Fig. 5. Performance of the output of the last two equations from Table 3: Eq. (10) by using just $E_{estimate}$ (age as symbol, smaller symbols and dotted lines) and Eq. (11) by using both $E_{estimate}$ and 'age' (larger symbols and solid lines) shown here versus E_{exper}. Least square regressions with their 95% confidence intervals. Note that although the two extremes are occupied by the oldest (92 year) and youngest specimens (35 year) the in between data is in random order with respect to the age of the individual and the second softest bone was in fact that of the 46 year old. Eq. (11) describes the Young's modulus irrespective of age and in fact even when one of the two extremes (i.e. the 92 year) datum is excluded from the analysis the R^2 falls only marginally from 0.94–0.91 showing that the analysis is robust.

between Eqs. (10) and (11). In Fig. 5 we show more clearly the performance of the predictions of the last two Eqs. (10) and (11) against the measured bending modulus values.

4. Discussion

This study utilised nano-indentation to investigate the mechanical properties of the microstructure of bone of various ages from the mid-femoral diaphyses of male donors. Unlike the more conventional microhardness techniques, nano-indentation provides both modulus of elasticity and hardness estimates for a material and can be used to target specifically various bone tissue structures at a microscopic level. In the present work nano-indentation was used to provide in human samples of various ages an appreciation of how bone achieves its bulk properties in a 'composite' sense.

We were particularly concerned with two structural elements: (a) the secondary osteons and (b) the interstitial bone matrix surrounding these osteons. Although we have carried out this work with the prior experience and knowledge we obtained in our previous (Rho et al., 1997, 1999) and other recent studies (Zysset et al., 1999) there were a number of limitations still present. Effects caused by a variable level of hydration of the tissue (Rho and Pharr, 1999) were of concern and so we performed all our nano-indentations on dry specimens. To minimise preparation artefacts we always used the same loading-time sequence, we tested at a site set at a reasonably chosen distance from the centre of the osteon, and mounted all sections in one and the same resin block. So, we have examined all samples from all donors under identical testing conditions. Although due to various restraints related to applying the nano-indentation method, the technique does not necessarily yield absolute values for the interrogated structures; nano-indentation ought to show us relative trends we seek to establish.

There were consistent differences between the stiffnesses of osteonal and interstitial bone. The interstitial bone was on average 2.3 GPa stiffer than the osteonal bone. Significant differences were also observed in the micromechanical properties of these two types of tissue between the different individuals. We have not observed any clear difference between the nano-indentation properties of younger and older bone, but the standard error of our slopes were in general so large, that all we can say at the moment is there is no evidence for any change. This may, to some extent, be a consequence of the small sample size of nine individuals. However, two other recent independent studies by Hoffler et al. (2000a, b) also produced elastic moduli and hardness of lamellae that were unrelated to age, gender and body mass index. Hoffler et al. (2000a) concluded, that since bone matrix elastic modulus and hardness is independent of age, gender and body mass index, reductions in the mechanical integrity of whole bone must be due to other factors like changes in tissue mass and organisation. The present study confirmed that this is the case by combining the results at the bone matrix level with histomorphometric variables like the level of porosity and the relative amount of secondary to interstitial tissue areas. In a related recent study (Zioupos and Currey, 1998), which provided the sample sections for the present study, we have also observed several strong correlations of the whole bone strength and toughness with age. The same work (Zioupos and Currey, 1998) showed that modulus was closely related to strength and toughness. This may, by implication mean that many of these other changes are also caused by structural and histological features than alterations in the bone matrix itself and this warrants further investigation.

The present analysis utilised Young's modulus obtained in bending where the stress field is neither uniform nor homogenous. However, the actual modulus values and its trends were consistent and very similar to other data already reported in the literature, especially with respect to variations across ages. The

combined composite 'rule of mixtures' approach showed that nano-data can be made to predict the elastic modulus of the whole bone of the various donors starting from the properties of the individual constituent structures. It is also worth pointing out, that it was not the absolute value of the composite modulus that we sought to establish, but its trends versus the nano-data and the structural data. It is obvious that there are other factors not accounted for, such as the interfibrillar and interlamellar degree of adhesion, the interfaces between secondary osteons, interstitial areas and other remnants of primary osteons or fibrolamellar bone. All these may indeed influence the bending modulus and explain some of the remaining 12% of variance, that is currently not accounted for (Eq. (10), Table 3).

In general, the variations we have recorded here in elastic modulus at the bone matrix level are generally small. The elastic modulus ranged between 21.5 and 25.4 GPa (least 85% of greatest) in interstitial sites, and 18.6 and 23.6 GPa (least 79% of greatest) in osteonal bone. Proportionally, these extremes are much less different than the variations in strength and toughness found by (Zioupos and Currey, 1998; Zioupos et al., 1999), which decline impressively with age (as much as by 45% for the 'work of fracture' over the same age range). It should be remembered that these measurements were also carried out on the *same* bones we used here and we believe that knowledge of the changes that occur in bone with ageing and between individuals is essential to understanding how, and perhaps why, these changes come about. Establishing natural age and/or donor-related changes in bone may also be important to understanding more serious forms of osteoporosis and other pathologic metabolic bone diseases and may be of a directly applied interest in the study of loosening and failure of artificial joints. A baseline of data of naturally occurring changes in bone and methods of interpolating between the data are needed to grasp and appreciate these biological aspects of bone mechanics and the present study has demonstrated that this may just be possible.

Acknowledgements

J.Y. Rho acknowledges the financial support of: the Whitaker Foundation, NIH -AR45297, Div. Mater. Sci. US DE -AC05-96OR22464/Lockheed Martin Energy Corp., and US DE -AC05-76OR00033/Oak Ridge and Assoc. Universities. P. Zioupos acknowledges the support of the EPSRC (GR/M59167, GR/N33225) and the efforts of Keith Winwood and Robert Kimber. J.D. Currey acknowledges the support of the Wellcome Trust (040350/Z/94/Z/MP/HA).

References

Ashman, R.B., Rho, J.Y., 1988. Elastic moduli of trabecular bone material. Journal of Biomechanics 21, 177–181.

Ashman, R.B., Rho, J.Y., Turner, C.H., 1989. Anatomical variation of the orthotropic elastic properties of the proximal human tibia. Journal of Biomechanics 22, 895–900.

Bailey, A.J., Paul, R.G., Knott, L., 1999. Mechanisms of maturation and aging of collagen. Mechanisms of ageing and Development 106, 1–56.

Bloebaum, R.D., Skedros, J.G., Vajda, E.G., Bachus, K.N., Constantz, B.R., 1997. Determining mineral content variations in bone using backscattered electron imaging. Bone 20, 485–490.

Boyce, T.M., Bloebaum, R.D., 1993. Cortical aging differences and fracture implications for the human femoral neck. Bone 14, 769–778.

Burstein, A.H., Reilly, D.T., Martens, M., 1976. Aging of bone tissue: mechanical properties. Journal of Bone and Joint Surgery 58A, 82–86.

Chakkalakal, D.A., Lippiello, L., Wilson, R.F., Shindell, R., Connolly, J.F., 1990. Mineral and matrix contributions to rigidity in fracture healing. Journal of Biomechanics 23, 425–434.

Courtney, A.C., Hayes, W.C., Gibson, L.J., 1996. Age-related differences in post-yield damage in human cortical bone: experiment and model. Journal of Biomechanics 29, 1463–1471.

Currey, J.D., 1982. 'Osteons' in biomechanical literature. Journal of Biomechanics 15, 717.

Currey, J.D., 1988. The effect of porosity and mineral content on the Young's modulus of elasticity of compact bone. Journal of Biomechanics 21, 131–717139.

Currey, J.D., Brear, K., Zioupos, P., 1996. The effects of aging and changes in mineral content in degrading the toughness of human femora. Journal of Biomechanics 29, 257–260.

Evans, F.G., 1976. Mechanical properties and histology of cortical bone from younger and older men. The Anatomical Record 185, 1–12.

Grynpas, M., 1993. Age and disease-related changes in the mineral of bone. Calcified Tissue International 53 (Suppl.1), S57–S64.

Hengsberger, S., Kulik, A., Zysset, Ph., 2000. A combined AFM and nano-indentation technique to measure the elastic properties of single bone lamellae under physiological conditions. In Proceedings 12th Conference European Society of Biomechanics, Dublin, 28-30 August 2000, p. 36.

Hoffler, C.E., Moore, K.E., Kozloff, K., Zysset, P.K., Goldstein, S.A., 2000a. Age, gender and bone lamellae elastic moduli. Journal of Orthopaedic Research 18, 432–437.

Hoffler, C.E., Moore, K.E., Kozloff, K., Zysset, P.K., Brown, M.B., Goldstein, S.A., 2000b. Hetergoeneity of bone lamellar-level elastic moduli. Bone 26, 603–609.

Katz, J.L., Meunier, A., 1993. Scanning acoustic microscope studies of the elastic properties of osteons and osteon lamellae. Journal of Biomechanical Engineering 115, 543–548.

Lindahl, O., Lindgren, Å.G.H., 1967. Cortical bone in man—II. Variation in tensile strength with age and sex. Acta Orthopaedica Scandinavica 38, 141–147.

Martin, B., 1993. Aging and strength of bone as a structural material. Calcified Tissue International 53 (Supp 1), S34–S40.

Martin, R.B., Boardman, D.L., 1993. The effects of collagen fiber orientation, porosity, density, and mineralization on bovine cortical bone bending properties. Journal of Biomechanics 26, 1047–1054.

McCalden, R.W., McGeough, J.A., Barker, M.B., Court-Brown, C.M., 1993. Age-related changes in the tensile properties of cortical bone: the relative importance of changes in porosity, mineralization

and microstructure. Journal of Bone and Joint Surgery 75A, 1193–1205.

Oliver, W.C., Pharr, G.M., 1992. An improved technique for determining hardness and elastic modulus using load and displacement sensing indentation experiments. Journal of Materials Research 7, 1564–1583.

Rho, J.Y., Pharr, G.M., 1999. Effects of drying on the mechanical properties of bovine femur measured by nanoindentation. Journal of Materials Science: Materials in Medicine 10, 485–488.

Rho, J.Y., Ashman, R.B., Turner, C.H., 1993. Young's modulus of trabecular bone material: ultrasonic and microtensile measurements. Journal of Biomechanics 26, 111–119.

Rho, J.Y., Tsui, T.Y., Pharr, G.M., 1997. Elastic properties of human cortical and trabecular lamellar bone measured by nanoindentation. Biomaterials 18, 1325–1330.

Rho, J.Y., Zioupos, P., Currey, J.D., Pharr, G.M., 1999. Variations in the individual lamellar properties within osteons by nanoindentation. Bone 25, 295–300.

Rho, J.Y., Roy, M., Pharr, G.M., 2000. Comments on 'Elastic modulus and hardness of cortical and trabecular bone lamellae by nano-indentation in the human femur'. Journal of Biomechanics 3, 1335.

Simmons, E.D., Pritzker, K.P.H., Grynpas, M.D., 1991. Age-related changes in the human femoral cortex. Journal of Orthopaedic Research 9, 155–167.

Skedros, J.G., Bloebaum, R.D., Bachus, K.N., Boyce, T.M., Constantz, B., 1993. Influence of mineral content and composition on greylevels in backscattered electron images of bone. Journal of Biomedical Materials Research 27, 57–64.

Smith, C.B., Smith, D.A., 1976. Relations between age, mineral density and mechanical properties of human femoral compacta. Acta Orthopaedica Scandinavica 47, 496–502.

Wall, J.C., Chatterji, S.K., Jeffery, J.W., 1979. Age–related changes in the density and tensile strength of human femoral cortical bone. Calcified Tissue International 27, 105–108.

Yamada, H., 1970. Mechanical properties of locomotor organs and tissues. In: Evans, F.G. (Ed.), Strength of biological materials. Williams and Wilkins, Baltimore, pp. 74–77.

Zioupos, P., 2001. Ageing human bone: factors affecting its biomechanical properties and the role of collagen. Journal of Biomaterials Applications 15, 187–229.

Zioupos, P., Currey, J.D., 1998. Changes in the stiffness, strength, and toughness of human cortical bone with age. Bone 22, 57–66.

Zioupos, P., Wang, X.T., Currey, J.D., 1996. The accumulation of fatigue-microdamage in human cortical bone of two different ages in-vitro. Clinical Biomechanics 11, 365–375.

Zioupos, P., Currey, J.D., Hamer, A.J., 1999. The role of collagen in the declining mechanical properties of aging human cortical bone. Journal of Biomedical Materials Research 45, 108–116.

Zysset, P.K., Guo, X.E., Hoffler, C.E., Moore, K.E., Goldstein, S.A., 1999. Elastic modulus and hardness of cortical and trabecular bone lamellae measured by nano-indentation in the human femur. Journal of Biomechanics 32, 1005–1012.

Zysset, P.K., Guo, X.E., Hoffler, C.E., Moore, K.E., Goldstein, S.A., 2000. Author's response 'Elastic modulus and hardness of cortical and trabecular bone lamellae measured by nano-indentation in the human femur'. Journal of Biomechanics 33, 1337.